

First-principles calculation of the instability leading to giant inverse magnetocaloric effects

D. Comtesse,¹ M. E. Gruner,¹ M. Ogura,² V. V. Sokolovskiy,^{3,4} V. D. Buchelnikov,⁴ A. Grünebohm,¹ R. Arróyave,⁵ N. Singh,⁶ T. Gottschall,⁷ O. Gutfleisch,⁷ V. A. Chernenko,⁸ F. Albertini,⁹ S. Fähler,¹⁰ and P. Entel^{1,*}

¹*Faculty of Physics and Center for Nanointegration, CENIDE,
University of Duisburg-Essen, D-47048 Duisburg, Germany*

²*Department of Physics, Graduate School of Science, Osaka University,
Machikaneyama 1-1, Toyonaka, Osaka 560-0043, Japan*

³*National University of Science and Technology, 'MIS&S', 119049 Moscow, Russia*

⁴*Condensed Matter Physics Department, Chelyabinsk State University, 454021 Chelyabinsk, Russia*

⁵*Department of Materials Science and Engineering,
Texas A&M University, College Station, Texas 77843, USA*

⁶*Department of Engineering Technology, University of Houston, Houston, Texas 77204, USA*

⁷*Materials Science, Technical University Darmstadt, D-64287 Darmstadt, Germany*

⁸*BCMaterials, University of Basque Country (UPV/EHU) and Ikerbasque,
Basque Foundation for Science, Bilbao 48011, Spain*

⁹*IMEM-CNR, Parco Area delle Scienze 37/A, I-43124 Parma, Italy*

¹⁰*IFW Dresden, P. O. Box 270116, D-01171 Dresden, Germany*

(Dated: February 3, 2014)

The structural and magnetic properties of functional Ni-Mn-Z ($Z = \text{Ga, In, Sn}$) Heusler alloys are studied by first-principles and Monte Carlo methods. The *ab initio* calculations give a basic understanding of the underlying physics which is associated with the strong competition of ferro- and antiferromagnetic interactions with increasing chemical disorder. The resulting *d*-electron orbital dependent magnetic ordering is the driving mechanism of magnetostructural instability which is accompanied by a drop of magnetization governing the size of the magnetocaloric effect. The thermodynamic properties are calculated by using the *ab initio* magnetic exchange coupling constants in finite-temperature Monte Carlo simulations, which are used to accurately reproduce the experimental entropy and adiabatic temperature changes across the magnetostructural transition.

PACS numbers: 75.50.-y, 75.10.-b, 75.30.Sg

Following the concepts of Hume-Rothery the influence of composition on martensitic and magnetic transformation temperatures is commonly condensed as a dependency of electrons per atom (e/a -ratio) [1]. Experiment and first-principles calculations, however, reveal that the Z element in Ni-Mn-Z Heusler alloys ($Z = \text{Ga, In, Sn}$) also affects the transformation temperatures substantially [2]. Moreover, recent experiments on samples with identical composition but different heat treatment indicate that chemical disorder also plays an important role [3–5]. Here, we use first-principles calculations to identify the influence of chemical disorder on the magnetic exchange parameters and derive guidelines for a further systematic improvement of magnetocaloric materials [6].

Besides the magnetocaloric effect (MCE) in Gd and other alloys at room temperature [7, 8], the metamagnetic Ni-Mn based Heusler materials [9, 10], have attracted much interest recently [11, 12]. In these alloys the metamagnetic features are responsible for magnetic glass behavior and frustration due to chemical disorder [13–15] as well as unusual magnetization behavior under an external magnetic field such as a large jump of the magnetization $\Delta M(T_m)$ at the martensitic/magnetostructural transformation temperature T_m [16]. This gives rise to the large inverse MCE of the materials [9, 10, 17, 18]. The

MCE can be influenced when Ni is substituted in part by Co: It is strongly enhanced in the case of In-based intermetallics [19, 20] (with adiabatic temperature change $\Delta T_{ad} = -6$ K in 2 T field [20]) while in the case of Ga the MCE is turned from direct to inverse by decoupling T_m and Curie temperature T_C [21] (with $\Delta T_{ad} = -1.6$ K in 1.9 T field [22, 23]).

Chemical disorder in the Mn-rich Heusler alloys is responsible for competing magnetic interactions (ferromagnetic versus antiferromagnetic) because the extra Mn atoms occupy lattice sites of the Z-sublattice which interact antiferromagnetically with the Mn atoms on the Y-sublattice due to RKKY-type interactions. This competition of magnetic interactions leads to the characteristic drop of magnetization curves at T_m , which is observed in Ni-(Co)-Mn-Z materials [14–16, 19–23]. (The magnetostructural transformation was originally discussed for Ni-excess Ni-Mn-Ga alloys which was interpreted as magnetic dilution effect [24].)

Previously, Monte Carlo (MC) methods [17, 18] and first-principles tools [25–27] have been used to explore the phase diagram and magnetostructural transformation of the magnetocaloric materials as a function of temperature and e/a [2, 28].

In this letter we show that basically the magnetic ex-

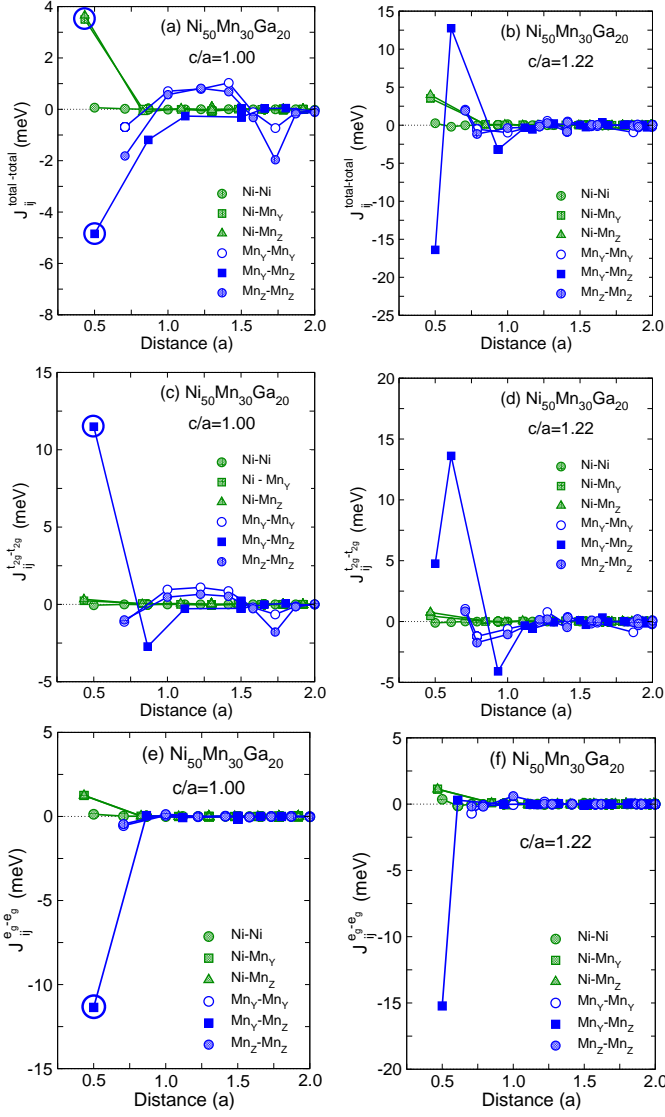


FIG. 1: (a-f) Element and orbital resolved magnetic exchange parameters of austenite and martensite $\text{Ni}_{50}\text{Mn}_{30}\text{Ga}_{20}$ from *ab initio* calculations (not all contributions are shown). It is obvious that the effect of ferromagnetic interactions is largely compensated by the influence of the antiferromagnetic interactions. (Austenite: $a = 5.85 \text{ \AA}$, martensite: $a = b = 5.47 \text{ \AA}$, $c = 6.68 \text{ \AA}$, $c/a = 1.22$.)

change interactions obtained from first-principles calculations allows to calculate the MCE as a function of temperature across the magnetostructural transition.

Before addressing the MCE, we would like to highlight the complex magnetic behavior of the disordered Ni-(Co)-Mn-Z alloys with excess Mn. We evaluate the effective exchange coupling constants J_{ij} using the KKR CPA method [26, 27] where, following the prescription of [29], the J_{ij} are obtained from

$$J_{ij} = \frac{1}{4\pi} \int_{-\infty}^{\epsilon_F} dE \text{Im Tr} \left[\Delta_i \tau_{\uparrow}^{ij} \Delta_j \tau_{\downarrow}^{ji} \right], \quad (1)$$

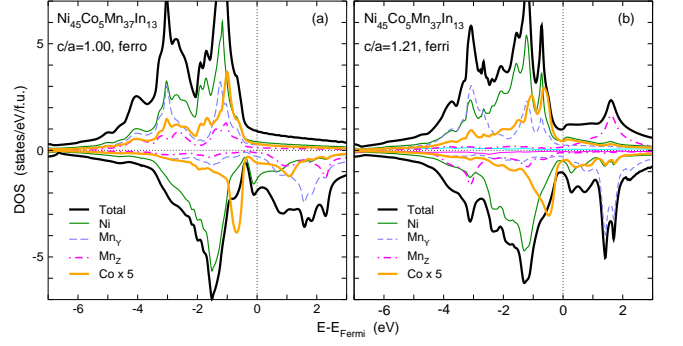


FIG. 2: Element resolved density of states of (a) austenite ($L2_1$, $a = 5.96 \text{ \AA}$) and (b) martensite ($L1_0$, $a = b = 5.6 \text{ \AA}$, $c = 6.76 \text{ \AA}$, $c/a = 1.21$) of $\text{Ni}_{45}\text{Co}_5\text{Mn}_{37}\text{In}_{13}$ showing the stabilization of martensite due to the formation of a pseudogap at E_F (“ferri” means that the spin of Mn on the In sites is reversed).

where Δ_i is the difference in the inverse single-site scattering t -matrices for spin-up and spin-down states, $\Delta_i = t_{i\uparrow}^{-1} - t_{i\downarrow}^{-1}$, and τ is the scattering path operator. Since we use the spherical potential and scalar relativistic approximation, the t -matrices are diagonal. Thus, we can decompose the J_{ij} and extract the contribution between L states ($L = (l, m)$ indicates the set of angular momentum and magnetic quantum number) at the i -th site and L' states at the j -site as

$$J_{ij}^{L-L'} = \frac{1}{4\pi} \int_{-\infty}^{\epsilon_F} dE \text{Im} \Delta_{iL} \tau_{\uparrow LL'}^{ij} \Delta_{jL'} \tau_{\downarrow L'L}^{ji}. \quad (2)$$

This allows to calculate element as well as orbital resolved magnetic coupling constants as shown, e.g., in Fig. 1 for disordered, non-stoichiometric $\text{Ni}_{50}\text{Mn}_{30}\text{Ga}_{20}$. (The effect of disorder on martensitic transformation has also been discussed by [30].)

From the behavior of the magnetic coupling constants in Fig. 1 for austenite and martensite $\text{Ni}_{50}\text{Mn}_{30}\text{Ga}_{20}$ as a function of the distance between the atoms we notice the nearly perfect compensation of ferromagnetic interactions associated with the more itinerant d -electron t_{2g} states and antiferromagnetic interactions of magnetic moments associated with the more localized e_g states. This destabilizes ferromagnetic austenite which undergoes a magnetostructural transformation to paramagnetic martensite (after addition of Co [21]). The magnetic exchange coupling constants of tetragonally distorted martensite ($c/a = 1.22$) cannot stabilize ferromagnetic order any more. In the MC simulations we use the magnetic exchange parameters from the zero-temperature *ab initio* calculations for austenite and martensite which we let merge at T_m . Thermal spin fluctuations will further help to stabilize the “paramagnetic” gap at $T < T_m$ below the magnetic jump $\Delta M(T_m)$ [22, 23]. This shows that the martensitic/magnetostructural instability is to a large extent

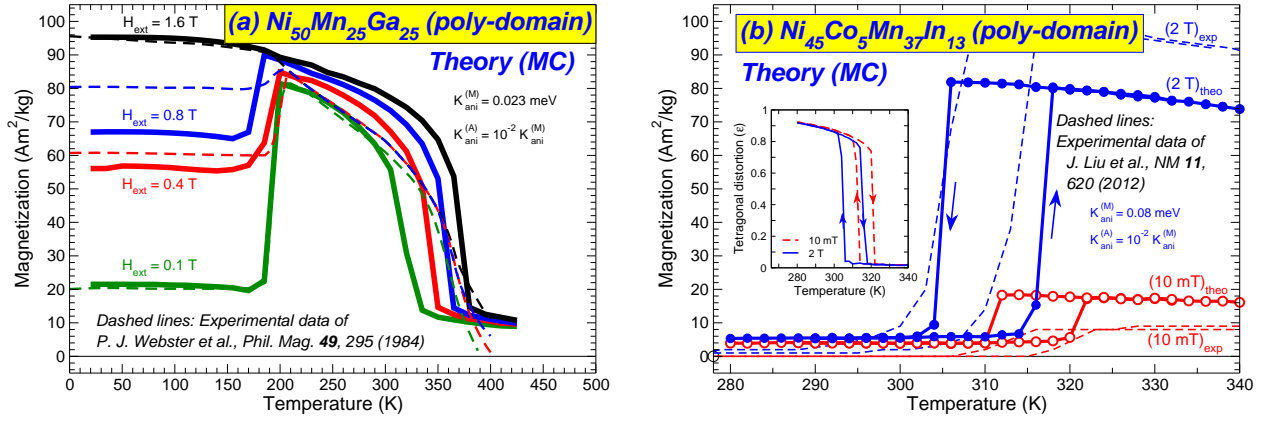


FIG. 3: (a) Monte Carlo magnetization curves (solid lines) of $\text{Ni}_{50}\text{Mn}_{25}\text{Ga}_{25}$ from the Potts model using *ab initio* magnetic exchange and magnetocrystalline anisotropy parameters, in comparison with experiment [34]. The jump of the magnetization curves vanishes for sufficiently large fields. (b) Theoretical and experimental magnetization curves of $\text{Ni}_{45}\text{Co}_5\text{Mn}_{37}\text{In}_{13}$ in a small and large external magnetic field of 10 mT and 2 T [20]. Here, the jump ΔM does not vanish for increasing magnetic fields. The inset shows the hysteresis from the first-order cubic-tetragonal transformation.

driven by the atomic disorder leading to strong competition of ferro- and antiferromagnetic interactions of approximately equal strength. This is responsible for the breakdown of ferromagnetic order in austenite and the appearance of the “paramagnetic gap” below T_m in martensite.

We emphasize that the same scenario works in case of Ni-(Co)-Mn-(In, Sn). With addition of Co (Co is likely to replace Ni because of similar coordination chemistry), the ferromagnetic tendencies increase but also the “disordered nature” of the magnetic interactions, which governs the magnetostructural instability. Although, Co leads to a decrease of T_m , it clearly has a favorable effect regarding the magnetocaloric properties. This is because Co hybridizes strongly with Ni states (see Fig. 2) and causes more spin disorder in the Heusler materials which leads to larger magnetic entropy and adiabatic temperature changes. (Note that competing interactions have also been discussed for Ni-Mn-Ga in [31, 32].)

The jump $\Delta M(T_m)$ which is accompanied by breakdown of long-range ferromagnetism, large magnetic fluctuations and a large entropy change across the magnetostructural transition, is at the heart of the giant inverse MCE.

Regarding thermodynamic properties we use the Blume-Emery-Griffiths (BEG) model [33] for austenite-martensite transformation in combination with the Potts model for the magnetic part and a magnetoelastic interaction term [17, 18]: $\mathcal{H} = \mathcal{H}_m + \mathcal{H}_{el} + \mathcal{H}_{int}$ where

$$\mathcal{H}_m = - \sum_{\langle ij \rangle} J_{i,j} \delta_{S_i, S_j} - g\mu_B H_{ext} \sum_i \delta_{S_i, S_g} M_i$$

$$+ K_{ani} \sum_i \delta_{S_i, S_k} M_i^2, \quad (3)$$

$$\begin{aligned} \mathcal{H}_{el} = & - \sum_{\langle ij \rangle} \sigma_i \sigma_j \left(J + U_1 g\mu_B H_{ext} \sum_i \delta_{\sigma_i, \sigma_g} \right) \\ & - K \sum_{\langle ij \rangle} (1 - \sigma_i^2) (1 - \sigma_j^2). \end{aligned} \quad (4)$$

The $J_{i,j}$ are the magnetic exchange parameters for each structure. Since mapping of *ab initio* energies is only onto J_{ij} with unit length of spins, field terms must include explicitly M_i , M_i^2 , where M_i is the *ab initio* value of magnetization of atom at site i taken to be dimensionless. J and K are the elastic and U_1 ($U_{i,j}$) the magnetoelastic interaction parameters (\mathcal{H}_{int} couples $M_i M_j$ and σ_i^2 , σ_j^2 with strength U_{ij} [17, 33]). The Kronecker symbol restricts the spin-spin interactions to those between the same Potts- q states. The spin moment of Mn is $S = \frac{5}{2}$ and we identify the $2S + 1$ spin projections with $q_{Mn} = 1 \dots 6$. Likewise, we assume $S = 1$ for Ni and $S = \frac{3}{2}$ for Co. The BEG model defines $\sigma_i = 0, \pm 1$ for austenite and two martensitic variants, respectively [17, 18, 33]; it allows first-order martensitic phase transformation with thermal hysteresis for sufficiently large biquadratic elastic interaction ($0.2 < K/J < 0.37$; we have adopted 0.23 for Ni-(Co)-Mn-In alloys). Because of the magnetoelastic coupling term the jump $\Delta M(T_m)$ is coupled to the martensitic transformation and exhibits hysteresis as well.

We mimic the magnetic aspect of polycrystalline materials by magnetic domain blocks with random initial spin configurations in each domain. The spins from different domain blocks can interact with probability $W = \min(1, \exp(-|K_{ani}|M_i^2/g\mu_B H_{ext}|M_i|))$. This stochastic competition between the magnetic anisotropy field and external magnetic field allows to realize experimental

trends of magnetization curves, see Fig. 3.

Hence, the extended Potts model in Eqs. (3-4) allows us to describe magnetic, structural as well as coupled magnetostructural phase transitions [17, 18]. Figure 3 shows magnetization curves in small and large magnetic fields for polycrystalline $\text{Ni}_{50}\text{Mn}_{25}\text{Ga}_{25}$ and $\text{Ni}_{45}\text{Co}_5\text{Mn}_{37}\text{In}_{13}$ in comparison to experiment [20, 34].

Note that there is a distinctive difference between $M(T)$ of the two materials.

For ferromagnetic Ni-Mn-Ga alloys near stoichiometry the jump vanishes for sufficiently large magnetic field when overcoming the magnetocrystalline anisotropy in agreement with experiment [11, 12, 34]. However, the jump persists for the Mn-rich Ni-Co-Mn-(Ga, In, Sn) up to large magnetic fields [19–23] because of strong antiferromagnetic $\text{Mn}_Y\text{-Mn}_Z$ interactions competing with the ferromagnetic ones. Note that for $\text{Ni}_{45}\text{Co}_5\text{Mn}_{37}\text{In}_{13}$ magnetization jump and hysteretic behavior in Fig. 3(b) agree well with experiment [20].

Total energy calculations and MC simulations show that the magnetostructural instability observed in Mn-rich systems [14–16, 19–23] is accompanied by a transition from ferromagnetic austenite to ferromagnetic/paramagnetic martensite, although, zero-temperature energy differences, $(E_{ferro} - E_{ferr})$ may already become small in austenite (this is the case for $\text{Ni}_{50-x}\text{Co}_x\text{Mn}_{25+y}\text{Sn}_{25-y}$ at a critical Co concentration). Free energies are difficult to evaluate on an *ab initio* basis because of chemical disorder, softening of lattice vibrations in austenite and magnetic excitations, which is beyond the scope of the present paper.

The adiabatic temperature changes across Curie temperature (direct MCE) and across magnetostructural transformation (inverse MCE) are determined by the isothermal magnetic entropy change and total specific heat (sum of magnetic and lattice specific heat, where the latter part is taken from the Debye model). These quantities can be calculated from the relations:

$$\begin{aligned} \Delta T_{ad}(T, H_{ext}) &= -\mu_0 \int_0^{H_{ext}} dH' \frac{T}{C(T, H')} \left(\frac{\partial M}{\partial T} \right)_{H'} \\ &\approx -T \frac{\Delta S_{mag}(T, H_{ext})}{C(T, H_{ext})}, \end{aligned} \quad (5)$$

$$\Delta S_{mag}(T_m, H_{ext}) = \Delta M(T_m, H_{ext}) \left(\frac{dT_m}{dH_{ext}} \right)^{-1}, \quad (6)$$

$$\Delta T_{ad}(T, H_{ext}) = -T \frac{\Delta S_{mag}(T_m, H_{ext})}{C(T, H_{ext})} \Delta f(T, H_{ext}) \quad (7)$$

Here, $\Delta S_{mag}(T, H_{ext}) = S_{mag}(T, H_{ext}) - S_{mag}(T, 0)$ is the entropy difference for finite and zero field. We use the Maxwell relation in Eq. (5) for the direct MCE while for the inverse MCE at the first-order magnetostructural transition we use instead Eqs. (6) and (7) based on the Clausius-Clapeyron equation. ΔM and ΔS_{mag} are the

jump of magnetization and magnetic entropy, dT_m/dH_{ext} is the shift of structural phase transition in the magnetic field and $\Delta f(T, H_{ext})$ is the change of austenite fraction caused by a field change, and $C(T, H_{ext})$ is the total specific heat. In our calculations the value of dT_m/dH_{ext} was taken from experiment [20], whereas ΔM and Δf were obtained from MC simulations.

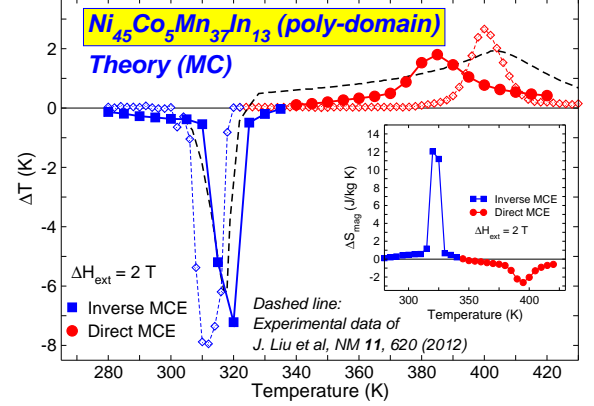


FIG. 4: Adiabatic temperature change of the direct (red circles) and inverse (blue squares) MCE of polycrystalline $\text{Ni}_{45}\text{Co}_5\text{Mn}_{37}\text{In}_{13}$ as obtained from the extended Potts model (diamonds: results for single-domain state; inset: temperature variation of the entropy).

Results for the MCE of Ni-Co-Mn-In alloys are shown in Fig. 4 which demonstrates the enhancement of cooling up to -6 K compared to samples without Co (≈ -3 K) [20]. The enhancement is caused by the increased magnetic disorder leading to larger $\Delta S_{mag}(T, H_{ext})$. However, systematic comparison is difficult because of either different sample preparation or compositions, compare, for instance, the different values reported for ΔS_{mag} and ΔT_{ad} regarding Ni-Mn-In alloys [19, 20, 35]. The key figure of merit in these alloys is large: we obtain $\text{RCP}_{inv} = -132$ J/kg for $\text{Ni}_{45}\text{Co}_5\text{Mn}_{37}\text{In}_{13}$.

In this paper we have shown that MCE is determined by the influence of competing ferromagnetic and antiferromagnetic interactions in Ni-Co-Mn-Z alloys [2]. The *ab initio* magnetic exchange parameters are the decisive parameters which determine the jump $\Delta M(T_m, H_{ext})$ and the size of the MCE. From the predictive power of *ab initio* calculations regarding the influence of the magnetic coupling constants to optimize the MCE, it might be worth to create even more spin disorder and larger isothermal entropy changes by looking for the effects of Cr and Gd added to Ni-Co-Mn-Z materials.

As already indicated by several experiments [1, 3–5] our calculations show that *e/a* ratios are not sufficient for describing the transformation behavior (like disorder broadened first-order magnetostructural phase transition, range of coexistence of phases and metastability [14–16, 36] and magnetic cluster formation [13]) and MCE in Heusler alloys completely. Though this con-

cept of itinerant electrons gives a rough overview on the transformation temperatures, the interaction of the localized electronic orbitals influences the exchange parameters and thus the size of the magnetocaloric effect. In particular, our calculations identify that it is beneficial having specific chemical environment for the Mn_Y and Mn_Z atoms since this optimizes the compensation of ferromagnetic and antiferromagnetic interactions. As chemical order is susceptible to time and temperature during the sample preparation in addition to composition, this guideline will allow for a systematic optimization of magnetocaloric materials.

We thank the DFG (SPP 1599) for financial support. RA and NS acknowledge support from NSF through Grants DMR-0844082 and 0805293.

* Electronic address: entel@thp.uni-duisburg.de

- [1] V. A. Chernenko, *Scripta Mater.* **40**, 523 (1999).
- [2] P. Entel, M. Siewert, M. E. Gruner, H. C. Herper, D. Comtesse, R. Arróyave, N. Singh, A. Talapatra, V. V. Sokolovskiy, V. D. Buchelnikov, F. Albertini, L. Righi, and V. A. Chernenko, *EPJB* **86**, 65 (2013).
- [3] W. Ito, Y. Imano, R. Kainuma, Y. Sutou, K. Oikawa, and K. Ishida, *Metall. Mater. Trans. A* **38**, 759 (2007).
- [4] S. Kustov, M. L. Corró, J. Pons, and E. Cesari, *Appl. Phys. Lett.* **94**, 191901 (2009).
- [5] R. Niemann, L. Schultz, and S. Fähler, *J. Appl. Phys.* **111**, 093909 (2012).
- [6] K. G. Sandeman, *Scripta Mater.* **67**, 566 (2012).
- [7] V. K. Pecharsky and K. A. Gschneidner, Jr. *Phys. Rev. Lett.* **78**, 4494 (1997).
- [8] O. Tegus, E. Brück, K. H. J. Buschow, and F. R. de Boer, *Nature* **415**, 150 (2002).
- [9] T. Krenke, E. Duman, M. Acet, E. F. Wassermann, X. Moya, L. Mañosa, and A. Planes, *Nature Mater.* **4**, 957 (2005).
- [10] R. Kainuma, Y. Imano, W. Ito, Y. Sutou, H. Morito, H. Okamoto, S. Kitakami, O. Oikawa, A. Fujita, T. Kanomata, and K. Ishida, *Nature* **439**, 957 (2006).
- [11] A. Planes, L. Mañosa, and M. Acet, *J. Phys.: Condens. Matter* **21**, 233201 (2009).
- [12] M. Acet, Ll. Mañosa, and A. Planes, in: *Handbook of Magnetic Materials*, vol. 19, edited by K. H. J. Buschow (Elsevier, Amsterdam, 2011). pp. 231-289.
- [13] K. P. Bhatti, S. El-Khatib, V. Srivastava, R. D. James, and C. Leighton, *Phys. Rev. B* **85**, 134450 (2012).
- [14] D. Y. Cong, S. Roth, and L. Schultz, *Acta Mater.* **60**, 5335 (2012).
- [15] A. Lakhani, A. Banerjee, P. Chaddah, X. Chen, and R. V. Ramanujan, *J. Phys.: Condens. Matter* **24**, 386004 (2012).
- [16] J. M. Barandiarán, V. A. Chernenko, E. Cesari, D. Salas, P. Lázpita, J. Gutiérrez, and I. Orue, *Appl. Phys. Lett.* **102**, 071904 (2013).
- [17] V. D. Buchelnikov, P. Entel, S. V. Taskaev, V. V. Sokolovskiy, A. Hucht, M. Ogura, H. Akai, M. E. Gruner, and S. K. Nayak, *Phys. Rev. B* **78**, 184427 (2008).
- [18] V. D. Buchelnikov, V. V. Sokolovskiy, S. V. Taskaev, V. V. Khovaylo, A. A. Aliev, L. N. Khanov, A. B. Batdalov, P. Entel, H. Miki, and T. Takagi, *J. Phys. D: Appl. Phys.* **44**, 064012 (2011).
- [19] D. Bourgault, J. Tillier, P. Courtois, D. Maillard, and X. Chauld, *Appl. Phys. Lett.* **96**, 132501 (2010).
- [20] J. Liu, T. Gottschall, K. P. Skokov, J. D. Moore, and O. Gutfleisch, *Nature Mater.* **11**, 620 (2012).
- [21] S. Fabbri, J. Kamarad, Z. Arnold, F. Casoli, A. Paoluzi, F. Bolzoni, R. Cabassi, M. Solzi, G. Porcari, C. Pernechele, and F. Albertini, *Acta Mater.* **59**, 412 (2011).
- [22] G. Porcari, S. Fabbri, C. Pernechele, F. Albertini, M. Buzzi, A. Paoluzi, J. Kamarad, Z. Arnold, and M. Solzi, *Phys. Rev. B* **85**, 024414 (2012).
- [23] G. Porcari, F. Cugini, S. Fabbri, C. Pernechele, F. Albertini, M. Buzzi, M. Mangia, and M. Solzi, *Phys. Rev. B* **86**, 104432 (2012).
- [24] V. V. Khovaylo, V. D. Buchelnikov, R. Kainuma, V. V. Koledov, M. Ohtsuka, V. G. Shavrov, T. Takagi, S. V. Taskaev, and A. N. Vasiliev, *Phys. Rev. B* **72**, 224408 (2005).
- [25] <http://cms.mpi.univie.ac.at/VASP/> (new release: VASP 5.3.3). G. Kresse and J. Furthmüller, *Phys. Rev. B* **54**, 11169 (1996).
- [26] *The Munich SPR-KKR package, version 6.3*, H. Ebert *et al.*, <http://olymp.cup.uni-muenchen.de/SPRKKR>. H. Ebert, D. Ködderitzsch, and J. Minár, *Rep. Prog. Phys.* **74**, 096501 (2011).
- [27] M. Ogura, C. Takahashi, and H. Akai, *J. Phys.: Condens. Matter* **19**, 365226 (2007).
- [28] M.A. Uijttewaal, T. Hickel, J. Neugebauer, M.E. Gruner, and P. Entel, *Phys. Rev. Lett.* **102**, 035702 (2009).
- [29] A. I. Liechtenstein, M. I. Katsnelson, V. P. Antropov, and V. A. Gubanov, *J. Magn. Magn. Mater.* **67**, 65 (1987).
- [30] H. B. Luo, C. M. Li, Q. M. Hu, S. E. Kulkova, B. Johansson, L. itos, and R. Yang *Acta Mater.* **59**, 5938 (2011).
- [31] I. Galanakis and E. Şaşıoğlu, *Appl. Phys. Lett.* **98**, 102514 (2011).
- [32] P. Lázpita, M. Barandiarán, J. M. Gutiérrez, J. Feuchtwanger, V. A. Chernenko, and M. R. Richard, *New J. Phys.* **13**, 033039 (2011).
- [33] T. Castan, E. Vives, and P.-A. Lindgard, *Phys. Rev. B* **60**, 7071 (1999).
- [34] P. J. Webster, K. R. A. Ziebeck, S. L. Town, and M. S. Peak, *Philos. Mag. B* **49**, 295 (1984).
- [35] X. Moya, L. Mañosa, A. Planes, S. Aksoy, M. Acet, E. F. Wassermann, and T. Krenke, *Phys. Rev. B* **75**, 184412 (2007).
- [36] L. H. Bennett, V. Provenzano, R. D. Shull, I. Levin, E. Della Torre, and Y. Jin, *J. All. Comp.* **525**, 34 (2012).